Macromolecules

COMMUNICATION TO THE EDITOR

pubs.acs.org/Macromolecules

Control of Crystal Morphology in Poly(L-lactide) by Adding Nucleating Agent

Hongwei Bai, Weiyi Zhang, Hua Deng,* Qin Zhang, and Qiang Fu*

College of Polymer Science and Engineering, State Key Laboratory of Polymer Materials Engineering, Sichuan University, Chengdu 610065, P. R. China

Supporting Information

1. INTRODUCTION

In the past few years, poly(L-lactide) (PLLA) has attracted increasing attention due to its excellent biocompatibility and processability.[1−3] As an eco-friendly thermoplastic polyester, PLLA can be produced completely from renewable sources, such as corn, and degrade into carbon dioxide and water in soil or a composting environment.[4−6] This sustainability makes PLLA a suitable alternative to traditional petrochemical-based polymers where their recycling still remains a challenge. PLLA has good mechanical properties at room temperature, such as high tensile strength and elastic modulus, but its article prepared by practical processing methods (e.g., injection molding) exhibits poor mechanical performance above its glass transition temperature (around 60 °C) since it remains almost amorphous after processing due to its slow crystallization rate.[7,8] Moreover, PLLA is brittle and its long-term behavior is poor because of a pronounced creep. The crystallization can restrict molecular mobility and then improve the long-term performance. Obviously, PLLA article with suitable crystallinity is required in many commercial applications. On the other hand, the mechanical, thermal properties, and even biodegradability of such semicrystalline polymer have been demonstrated to be strongly dependent on the crystal morphology and structure.[9−14] Therefore, the realization of effective control on the crystal superstructure consisting of crystalline lamella, such as spherulites and shish-kebab structure, is of great scientific and technical significance because it might provide a route to prepare PLLA products with excellent macroscopic performance.

In most cases, isotropic spherulite-like crystal morphology is observed for semicrystalline polymer including PLLA, while shish-like fibril crystals are often obtained from the sheared melt.[15−17] Many researchers reported that adding nucleating agent is a useful method for controlling the crystal superstructure of polymer, such as polyolefins.[10,13,18−21] For example, the exclusive formation of bundle-like superstructure for β-phase and the radiating, spherulitic superstructure for α-phase in polypropylene (PP) can be induced by adding highly active β-form and α-form nucleating agent, respectively.[10,13,18−20] Moreover, the assembled structure could vary with its concentration and the thermal conditions during melting and crystallization if the nucleating agent is partially or completely dissolved in the polymer melt and recrystallize during cooling. As a result, different superstructures of PP could be induced.[13,18−21] For instance, sorbitol-based nucleating agents, such as well-known 1,3:2,4-bis(3,4-dimethylbenzylidene)sorbitol (DMDBS), can self-organize into nanofibils on cooling, and then lateral growth of PP lamellae occurs orthogonally to the fibrils, forming a typical shish-kebab structure.[22] Thus, adding nucleating agent with the ability of self-organizing in polymer melt is believed to be an important method to manipulate crystal morphology as well as properties of polymer articles. Similar to DMDBS, 1,3,5-benzenetricarboxylamide derivatives, another family of nucleating agents for PP, are also found to be capable of self-organizing in PP melt through intermolecular hydrogen bonding of the amides in the form of a three-dimensional fibrillar network.[23−25] Very recently, the derivatives have been successfully used to enhance the crystallization of PLLA.[26] However, no attention has been paid to the self-organization of the derivatives in PLLA melt and its subsequent effect on the crystal morphology of PLLA though it is very important for the macroscopic performance. Therefore, in this Communication, we use one of the above derivatives, i.e., *N*,*N*′,*N*″-tricyclohexyl-1,3,5-benzenetricarboxylamide (TMC-328), as a model to tailor the crystal superstructure of PLLA, and three crystal morphologies including cone-like, shish-kebab, and needle-like structures have been successfully obtained for the first time using melt crystallization. Furthermore, the evolution of crystal morphology during crystallization is investigated using in-situ POM and rheological measurement.

2. EXPERIMENTAL SECTION

2.1. Materials and Sample Preparation. Commercially available PLLA (trade name 4032D, NatureWorks) with high stereoregularity (1.2−1.6% D-isomer lactide) was used in this study. It has a density of 1.25 g/cm^3. The weight-averaged molecular weight and polydispersity are 207 kDa and 1.74, respectively. The novel nucleating agent *N*,*N*′,*N*″-tricyclohexyl-1,3,5-benzenetricarboxylamide (TMC-328) with a melt temperature of about 375 °C was kindly supplied by Shanxi Provincial Institute of Chemical Industry, China. The chemical structure is shown in Supporting Information Figure S1.

To achieve desired loading and good dispersion of small amounts of nucleating agent (below 0.5 wt %) in PLLA, a master batch of 5 wt % TMC-328 in PLLA was first prepared using a corotating twin-screw extruder (TSSJ-25) at 170−190 °C, and

Received: October 26, 2010
Revised: January 14, 2011

then the master batch was diluted with PLLA in a Haake internal mixer (Rheomix 600) at 190 °C and 60 rpm for 6 min. For comparison, PLLA without nucleating agent was also processed with the same method. The concentrations of TMC-328 in PLLA were 0.05, 0.1, 0.2, 0.3, and 0.5 wt %. For convenience, they were denoted as a code of PLLA-*x*, where *x* indicates the weight percentage of TMC-328 in the system. Please note that both PLLA and TMC-328 were dried in a vacuum oven at 60 °C for 12 h before compounding.

2.2. Characterizations. Morphological observations of PLLA crystallites were conducted on a polarized optical microscopy (POM, Leica DMLP) equipped with a hot stage (Linkam THMS 600) under crossed polarizers. All samples were first inserted between two microscope coverslips and squeezed at 200 °C to obtain a slice with a thickness of around 20 μm. Subsequently, the as-prepared slice was transferred to the hot stage and held at 200 °C for 5 min to achieve thermal equilibrium. It is followed by rapid cooling to a selected crystallization temperature of 130 °C. The in-situ POM micrographs during isothermal crystallization were recorded by a Cannon digital camera.

The spin-coating method was applied to prepare the samples for atomic force microscopy (AFM) measurement. Thin films with a thickness of around 2 μm were obtained with spin-coating a chloroform solution of PLLA/TMC-328 (20 mg/mL) on a microscope coverslip (20 × 20 mm). After drying under vacuum oven at 60 °C for 12 h to remove residual solvent, the obtained thin films on the glass substrate were melted at 200 °C for 5 min on a hot stage (Linkam THMS 600) and then quickly quenched to 130 °C to allow an isothermal crystallization for several minutes. The measurement was performed in tapping mode with a commercial AFM (SPI4000/SPA400, Seiko Instruments). Both height and phase images were recorded simultaneously during scanning.

The rheological behavior of all samples were characterized using a stress-controlled rotational rheometer (AR2000ex, TA Instruments) with 25 mm diameter and 1 mm gap parallel plates. Before the measurement, each disk-shaped specimen prepared by compression molding was heated to 240 °C and held for 3 min to completely melt PLLA and TMC-328, and then it was subjected to a dynamic temperature sweep with −3 °C/min ramp to monitor the evolution of the storage modulus with temperature during nonisothermal crystallization. The applied stress and oscillation frequency were set at 10 Pa and 2 rad/s, respectively. All rheological measurements were performed under a nitrogen atmosphere to minimize degradation.

3. RESULTS AND DISCUSSION

3.1. Nucleated Crystallization of PLLA As Studied via DSC. Nucleating agent is often used to accelerate crystallization by decreasing nucleation barrier and increasing nucleation density. In order to identify the nucleation efficiency of TMC-328 in PLLA, isothermal and nonisothermal crystallization behaviors were investigated with DSC. The results indicate that TMC-328 acts as an effective nucleating agent for PLLA crystallization, but no extra nucleation effect can be obtained when its contents exceed 0.2 wt % (see Supporting Information Figure S2). In addition, it is noteworthy that the presence of TMC-328 can greatly enhance the crystallization of PLLA but has no influence on the crystalline modification. In all the cases, α-form crystal structure of PLLA is exclusively obtained (see Supporting Information Figure S3).

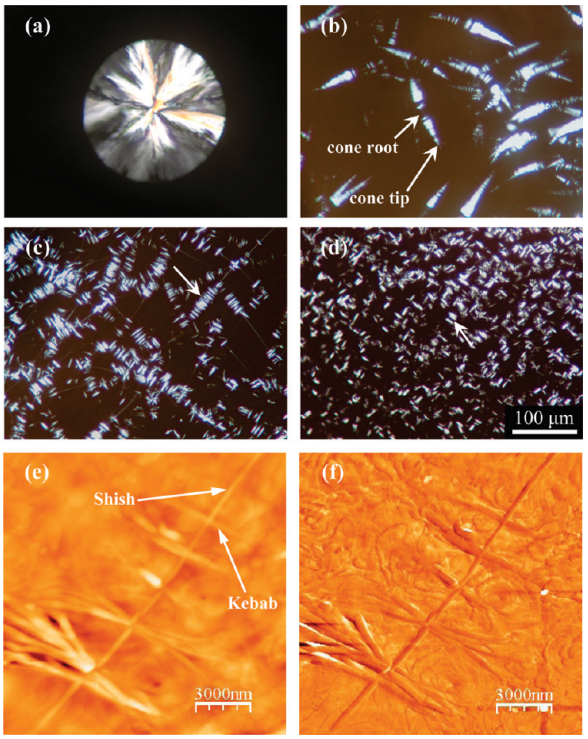

Figure 1. POM micrographs of the crystal morphology for PLLA-0 (a), PLLA-0.2 (b), PLLA-0.3 (c), and PLLA-0.5 (d) prepared by isothermal crystallization at 130 °C for 55, 7, 10, and 10 min, respectively. Image (a) shows a typical PLLA spherulitic morphology; image (b) shows macroscopic cone-like structure; but for images (c) and (d), macroscopic shish-kebab-like and needle-like structure are observed, respectively. AFM height (e) and phase (f) images of PLLA-0.2 show a typical shish-kebab-like superstructure. The sample was first produced by the spin-coating method and then crystallized isothermally at 130 °C.

It is well-known that the crystallization and resultant superstructure of semicrystalline polymers largely depend on the nucleation, especially the morphology of nucleating agent in polymer melt before crystallization.[9,13,18−20] For a given thermal condition during heating and cooling, the structural morphology is essentially determined by the concentration-dependent solubility of nucleating agent in polymer.[9,13,18−20] It is expected that the nucleating agent could be completely dissolved in polymer melt and self-associate into uniform structures upon cooling at relatively low concentrations. However, it may become partly insoluble in polymer melt at concentrations exceeding the solubility limit. In this case, the crystal morphology is largely dependent on the undissolved state (e.g., shape and size) of nucleating agent. In current study, the crystallization rate of PLLA are hardly affected by TMC-328 concentrations in the range of 0.2−0.5 wt %, but the self-associated morphology of TMC-328 in PLLA may be different with different TMC-328 concentrations, thus inducing various crystal superstructures in PLLA. Therefore, the morphology of TMC-328 and resultant superstructure of PLLA was investigated with POM, and the result is presented as follows.

3.2. Crystal Morphology of PLLA As Investigated via POM. The crystal morphology of PLLA was observed with POM, and the results are shown in Figure 1. As expected, a typical spherulitic morphology is observed for PLLA-0 (Figure 1a). However, the crystal morphology for nucleated PLLA is clearly different from that of PLLA-0 and dependent on the loading levels of TMC-328

dx.doi.org/10.1021/ma102439t |*Macromolecules* XXXX, XXX, 000–000

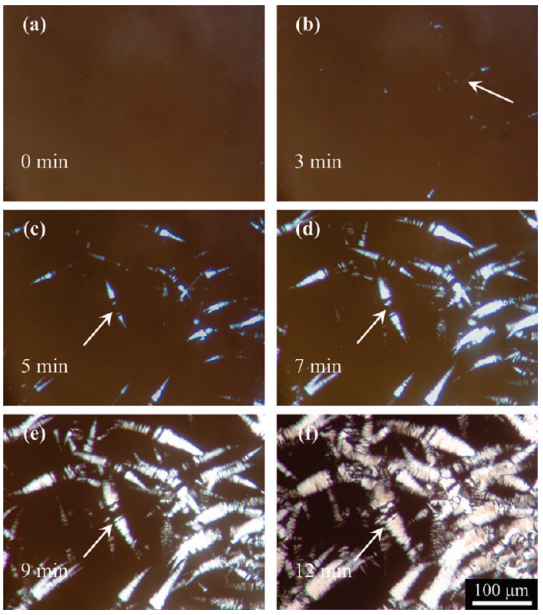

Figure 2. Time evolution of POM micrographs of crystal morphology for PLLA-0.2 during isothermal crystallization at 130 °C. The corresponding crystallization time is given in the profiles.

in PLLA. PLLA-0.3 presents a macroscopic shish-kebab-like structure, in which disk-shaped kebab-like structure is uniformly located on the surface of fine fibrils (serves as shish) with a length of hundreds of micrometers (Figure 1c). The fine fibrils can be formed through the self-organization of TMC-328, as demonstrated by in-situ POM observation and rheological measurement (see below). With further increase of TMC-328 concentration to 0.5 wt %, the length of shish becomes shorter and only needle-like morphology is observed (Figure 1d). It is interesting to note that the size of the disk-shaped kebab-like structure for PLLA-0.2 changes gradually from large to small along the long axis of the shish, and then a unique macroscopic cone-like structure is formed (Figure 1b). Moreover, the package density of PLLA lamellae around the cone tip appears to be much larger than those around its root. However, it is very difficult to identify individual kebab-like structure with POM; therefore, the detailed structure is characterized with AFM at a microscopic level. As shown in Figure 1e,f, AFM results illustrate that bundled lamellae are periodically decorated on the surface of the fibril with a diameter of around 300 nm for PLLA-0.2.

To reveal the nucleation in detail and subsequent evolution of the macroscopic crystal morphology during crystallization, in-situ POM measurement was performed. Shown as an example, Figure 2 shows the evolution of the macroscopic cone-like structure for PLLA-0.2 during isothermal crystallization at 130 °C. Obviously, no birefringence arising from the undissolved TMC-328 particles or their self-assembled structures is detected at the initial stage of crystallization (Figure 2a). However, some fine fibrils are observed as the crystallization time reaches 3 min (Figure 2b), indicating that TMC-328 can be dissolved in PLLA melt and recrystallizes during cooling. With further increasing crystallization time, more self-organized structure of TMC-328 molecules at the growth front is observed. It is followed by the growth of disk-shaped kebab-like structure on such self-organized fibrils surface (Figure 2c−f). Under this condition, the dimension of the disk-shaped kebab-like structure near the cone tip (growth front of the fibrillar structure) is smaller than that near the initially formed cone root as the growth time of the kebabs varies with their locations on shish surface. As a consequence, the unique cone-like structure is formed. Furthermore, the package density of kebab-like structure along the shish axis is not uniform; less closely packed kebab-like lamellae is observed around the cone root. It is probably due to the fact that the diameter of shish near the cone root is relatively larger than that near the cone tip. In contrast, for PLLA-0.3, TMC-328 self-associates into highly ordered fibrils in the melt rapidly before the onset of PLLA crystallization. Thus, the growth of PLLA bundled lamellae (kebab) is induced, forming a charming macroscopic shish-kebab-like structure, where the disk-shaped kebab-like structure is uniformly located along the shish axis (see Supporting Information Figure S4). Clearly, the evolution of crystal morphology is largely determined by the nucleation in PLLA-0.2 and PLLA-0.3. Once the formation of self-organized fibrils is achieved in the melt, PLLA lamellae begin to grow on their surface shortly. Nevertheless, the self-association rate of TMC-328 molecules in PLLA-0.2 is much lower than the crystallization rate of PLLA, causing the growth time of the kebabs is significantly different along the shish axis. On the contrary, the crystallization rate of TMC-328 is quite higher than that of PLLA in PLLA-0.3 due to the significant decreased solubility of TMC-328 with further increase in its concentration. The self-organization of fibrils is already completed prior to PLLA crystallization at 130 °C. This may be the main reason for the distinct crystal morphologies observed in PLLA-0.2 and PLLA-0.3. To further clarify the dependence of PLLA crystal morphology on the relative crystallization rate of PLLA and TMC-328, the evolution of the crystal morphology of PLLA in PLLA-0.3 is detected at 120 °C where the relative crystallization rate becomes faster compared with that at 130 °C due to the decreased self-organization rate of TMC-328 and increased crystallization rate of PLLA (see Supporting Information Figure S5). Obviously, in this case, disk-shaped kebabs can grow on the surface of the rapidly self-organized fibrils and thus form the macroscopic shish-kebab-like structure. However, with the further development of the fibrils, the unique cone-like structure is formed at their growth front (shown by the arrows), which is similar to that in PLLA-0.2. Very importantly, as the crystallization temperature further depresses to 110 °C, more cone-like structure can be observed in PLLA-0.3 due to the significant decrease in the self-organization rate of TMC-328 (see Supporting Information Figure S6a). The results suggest that the relative crystallization rate of the PLLA and TMC-328 determines the crystal morphology of PLLA. The shish-kebab-like structure can be obtained only if the relative crystallization rate of PLLA and TMC-328 is very slow. It can be well supported by the crystal morphology of PLLA-0.2 obtained at 140 °C, where the crystallization rate of TMC-328 is much higher than that of PLLA, disk-shaped kebabs grow slowly on the surface of the self-organized fibrils and then forms the shish-kebab-like structure (see Supporting Information Figure S6b).

The evolutions of the macroscopic crystal morphology for PLLA-0.5 during isothermal crystallization can be found in Supporting Information Figure S7. Obviously, TMC-328 is partly insoluble, and large amount of undissolved fibrillar structures is observed even in PLLA melt at 200 °C (Figure S7a). In this case, the self-organizing ability of TMC-328 deteriorates significantly upon cooling, and then the undissolved short fibrillar crystals instead of self-organized long fibrils serve as

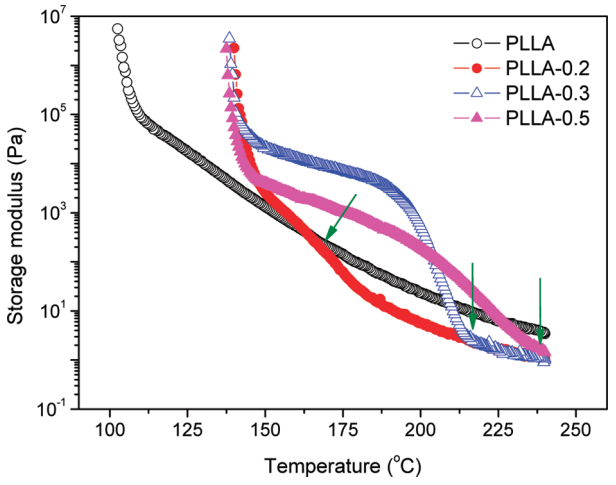

Figure 3. Evolution of storage modulus with temperature during crystallization at a cooling rate of 3 °C/min for the samples. The arrows represent the onset of TMC-328 phase separation on cooling which leads to a gel-like network of TMC-328 fibrils suspended in the PLLA melt.

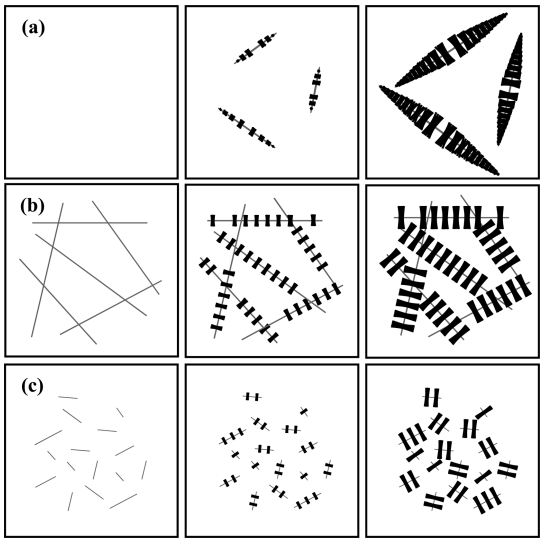

Figure 4. Schematic representation of the evolution of crystal morphologies during crystallization for nucleated PLLA with different loading levels of TMC-328: (a) PLLA-0.2, (b) PLLA-0.3, and (c) PLLA-0.5.

nucleation sites, inducing a needle-like structure of PLLA crystals. A similar concentration dependence of self-organized morphology of nucleating agent in polymer melt has been reported elsewhere for aryl amide derivative (TMB-5) nucleated PP by Dong et al.[18]

3.3. Crystallization Studied via Rheological Measurement. Rheological measurement is well-known to be very sensitive to the microstructural changes in polymers. It is frequently used to investigate the crystallization process of polymers.[13,20,21] Figure 3 shows the evolution of storage modulus (G') with temperature during crystallization from the melt for PLLA with or without TMC-328. For PLLA-0, it is clear that an approximately linear increase in storage modulus with decreasing temperature from 240 to 110 °C is observed due to the increased viscosity. A similar tendency is also obtained in the curve of complex viscosity vs temperature (not shown here). A sharp increase in G' at 110 °C is caused by the crystallization of PLLA. For PLLA-0.3, a sudden and dramatic increase in storage modulus is observed around 215 °C, which is far above the crystallization temperature of PLLA. This indicates the formation of a self-organized three-dimensional fibrillar network due to phase separation of TMC-328 molecules in PLLA melt.[20,21] In this case, crystallization occurs around 140 °C, as indicated by a sharp increase in storage modulus. With increasing concentration up to 0.5 wt %, TMC-328 phase separation shifts to a higher temperature. Furthermore, the level of G' for PLLA-0.5 is lower than that for PLLA-0.3 after the formation of the three-dimensional network. This can be explained by the difference in entanglement density in the two fibrillar networks. Comparing with short fibrils in PLLA-0.5 (as shown in Figure 1d), the self-organized long fibrils in PLLA-0.3 (as shown in Figure 1c) endow the network with higher entanglement density, thus leading to a stiffer fibrillar network. Regarding to PLLA-0.2, a step increase in G' is observed at 180 °C, but a rapid enhancement of G' dose not appears until the onset of PLLA crystallization. This suggests that only a fraction of TMC-328 molecules self-organize into some fine fibrils, and no stable physical network is formed upon cooling. The rheological measurement result suggests that the crystallization takes place around 140 °C for all the PLLA containing TMC-328 disregarding its concentration. This is consistent with the result obtained with DSC. It should be mentioned that the dissolved TMC-328 molecules in PLLA melt may act as a low-molecular-weight diluent at high temperatures, driving G' shift to lower values compared with neat PLLA.

3.4. Schematic Representation of the Evolution of Crystal Morphologies. Similar to the study previously reported for PP,[23−25] TMC-328 can be dissolved in PLLA melt and self-assemble through intermolecular hydrogen bonding of the amides upon cooling, leading to highly ordered fibrils with large surface capable of nucleating PLLA. Although the underlying mechanism of the nucleation is not well understood, it is widely accepted that polymer chains grow epitaxially on the surface of nucleating agent.[27] Lotz and co-workers[28,29] discussed the epitaxial growth of PP on the surface of various families of nucleating agents and proposed that the epitaxy matching between the two in terms of crystal structure and lattice parameters is required to obtain a highly active nucleating efficiency. Herein, PLLA and the self-organized fibrils of TMC-328 must have a matching structural feature. The fibrils serve as shish to promote epitaxial growth of kebab-like lamellae on their surface. The crystal morphology evolution of the nucleated PLLA with different loading levels of TMC-328 during crystallization is described schematically as shown in Figure 4. The morphology of TMC-328 in PLLA melt varies with the increase of its concentrations (0.2, 0.3, and 0.5 wt %), inducing three characteristic crystal morphologies, i.e., cone-like, shish-kebab-like, and needle-like macroscopic structure, respectively. It should be noted that the shish-kebab-like structure containing bundled lamellae as kebab observed in this study is definitely different from the conventional shish-kebab structure where lamellar single crystals are periodically located on the shish core. Furthermore, the package density of lamellae around shish in the latter is much larger than that in the former.

4. CONCLUSION

In summary, we have demonstrated that nucleating agent can be used to control the superstructure of PLLA effectively. Three

dx.doi.org/10.1021/ma102439t |*Macromolecules* XXXX, XXX, 000–000

unique crystal superstructures, including cone-like, shish-kebab-like, and needle-like structure, have been obtained for the first time by melt crystallization. In-situ POM and rheological measurements show that TMC-328 can be dissolved in PLLA melt and self-organize into fine fibrils prior to PLLA crystallization. And then, these fibrils serve as shish to induce the epitaxial growth of kebab-like structure approximately orthogonal to the long axis. Since the crystal superstructure is of great significance in polymer science and technology, this report is expected to prompt us to further explore the underlying formation mechanisms and exploit novel high-performance eco-friendly PLLA articles.

■ ASSOCIATED CONTENT

Supporting Information. DSC and WAXD measurements, chemical structure of the nucleating agent TMC-328, nucleated crystallization behaviors of PLLA measured from DSC, wide-angle X-ray diffraction patterns of the nucleated PLLA, time evolution of crystal morphology for PLLA-0.3 and PLLA-0.5 during isothermal crystallization at 130 °C, time evolution of crystal morphology for PLLA-0.3 during isothermal crystallization at 120 °C, and POM micrographs of crystal morphology for PLLA-0.3 and PLLA-0.2 isothermally crystallized at different temperatures. This material is available free of charge via the Internet at http://pubs.acs.org.

■ AUTHOR INFORMATION

Corresponding Author

*Tel/Fax +86 28 8546 1795, e-mail qiangfu@scu.edu.cn (Q.F.); e-mail Huadeng@scu.edu.cn (H.D.).

■ ACKNOWLEDGMENT

We express our sincere thanks to the National Natural Science Foundation of China for financial support (50903048, 50873063).

■ REFERENCES

(1) Lim, L. T.; Auras, R.; Rubino, M. *Prog. Polym. Sci.* **2008**, *33*, 820–852.
(2) Athanasiou, K. A.; Niederauer, G. G.; Agrawal, C. M. *Biomaterials* **1996**, *17*, 93–102.
(3) Lin, Y. M.; Boccaccini, A. R.; Polak, J. M.; Bishop, A. E. *J. Biomater. Appl.* **2006**, *21*, 109–118.
(4) Drumright, R. E.; Gruber, P. R.; Henton, D. E. *Adv. Mater.* **2000**, *12*, 1841–1846.
(5) Kale, G.; Auras, R.; Singh, S. P.; Narayan, R. *Polym. Test.* **2007**, *26*, 1049–1061.
(6) John, R. P.; Nampoothiri, K. M.; Pandey, A. *Process Biochem.* **2006**, *41*, 759–763.
(7) Mitomo, H.; Kaneda, A.; Quynh, T. M.; Nagasawa, N.; Yoshii, F. *Polymer* **2005**, *46*, 4695–4703.
(8) Tsuji, H.; Ikada, Y. *Polymer* **1995**, *36*, 2709–2716.
(9) Jiang, N.; Zhao, L. F.; Gan, Z. H. *Polym. Degrad. Stab.* **2010**, *95*, 1045–1053.
(10) Bai, H. W.; Wang, Y.; Song, B.; Huang, T.; Han, L. *J. Polym. Sci., Part B: Polym. Phys.* **2009**, *47*, 46–59.
(11) Gan, Z. H.; Kuwabara, K.; Abe, H.; Iwata, T.; Doi, Y. *Polym. Degrad. Stab.* **2005**, *87*, 191–199.
(12) Kristiansen, M.; Tervoort, T.; Smith, P.; Goossens, H. *Macromolecules* **2005**, *38*, 10461–10465.
(13) Luo, F.; Geng, C. Z.; Wang, K.; Deng, H.; Chen, F.; Fu, Q.; Na, B. *Macromolecules* **2009**, *42*, 9325–9331.
(14) Zhu, B.; He, Y.; Nishida, H.; Yazawa, K.; Ishii, N.; Kasuya, K.; Inoue, Y. *Biomacromolecules* **2008**, *9*, 1221–1228.
(15) Keum, J. K.; Zuo, F.; Hsiao, B. S. *Macromolecules* **2008**, *41*, 4766–4776.
(16) Somani, R. H.; Yang, L.; Zhu, L.; Hsiao, B. S. *Polymer* **2005**, *46*, 8587–8623.
(17) Yamazaki, S.; Itoh, M.; Oka, T.; Kimura, K. *Eur. Polym. J.* **2010**, *46*, 58–68.
(18) Dong, M.; Guo, Z. X.; Yu, J.; Su, Z. Q. *J. Polym. Sci., Part B: Polym. Phys.* **2009**, *47*, 314–325.
(19) Varga, J.; Menyhard, A. *Macromolecules* **2007**, *40*, 2422–2431.
(20) Kristiansen, M.; Werner, M.; Tervoort, T.; Smith, P.; Blomenhofer, M.; Schmidt, H. W. *Macromolecules* **2003**, *36*, 5150–5156.
(21) Shepard, T. A.; Delsorbo, C. R.; Louth, R. M.; Walborn, J. L.; Norman, D. A.; Harvey, N. G.; Spontak, R. J. *J. Polym. Sci., Part B: Polym. Phys.* **1997**, *35*, 2617–2628.
(22) Balzano, L.; Rastogi, S.; Peters, G. W. M. *Macromolecules* **2008**, *41*, 399–408.
(23) Blomenhofer, M.; Ganzleben, S.; Hanft, D.; Schmidt, H. W.; Kristiansen, M.; Smith, P.; Stoll, K.; Mader, D.; Hoffmann, K. *Macromolecules* **2005**, *38*, 3688–3695.
(24) Mohmeyer, N.; Behrendt, N.; Zhang, X. Q.; Smith, P.; Altstadt, V.; Sessler, G. M.; Schmidt, H. W. *Polymer* **2007**, *48*, 1612–1619.
(25) Kristiansen, P. M.; Gress, A.; Smith, P.; Hanft, D.; Schmidt, H. W. *Polymer* **2006**, *47*, 249–253.
(26) Nakajima, H.; Takahashi, M.; Kimura, Y. *Macromol. Mater. Eng.* **2010**, *295*, 460–468.
(27) Thierry, A.; Fillon, B.; Straupé, C.; Lotz, B.; Wittmann, J. C. *Prog. Colloid Polym. Sci.* **1992**, *87*, 28–31.
(28) Mathieu, C.; Thierry, A.; Wittmann, J. C.; Lotz, B. *Polymer* **2000**, *41*, 7241–7253.
(29) Mathieu, C.; Thierry, A.; Wittmann, J. C.; Lotz, B. *J. Polym. Sci., Part B: Polym. Phys.* **2002**, *40*, 2504–2515.